

轴向运动功能梯度梁横向振动问题的保结构分析*

刘涛¹ 周洋忻² 胡伟鹏^{2†}

(1. 榆林市城市投资经营集团有限公司, 榆林 719000) (2. 西安理工大学 土木建筑工程学院, 西安 710048)

摘要 轴向运动速度和材料的非均匀性对轴向运动功能梯度梁振动问题分析提出了严峻挑战. 本文在简要回顾轴向运动功能梯度梁横向振动动力学模型基础上, 基于无限维动力学系统的对称破缺理论和广义多辛分析方法, 构造了横向振动模型的保结构数值格式, 并在给定材料参数时给出了数值格式具有良好保结构性能的条件. 分别采用微分求积法、复模态法和保结构方法分析横向振动模型的前六阶频率, 发现保结构方法得到的频率结果与复模态法得到的结果吻合较好, 在此基础上分析了微分求积法的主要误差来源, 以指导微分求积法的改进, 并为复杂动力学系统的数值求解提供了新途径.

关键词 保结构, 轴向运动功能梯度梁, 对称破缺, 广义多辛, 横向振动

中图分类号: O302

文献标志码: A

引言

功能梯度材料由于控制界面的成分和组织连续变化, 使材料的热应力大为缓和, 而在航空航天、机械工程、生物医药等领域应用广泛^[1-3]. 智慧建造^[4]这一全新概念的提出, 使得传统单一均匀材料无法满足建筑设计工程的需求, 因此, 功能梯度材料将是未来实现很多智慧建造特殊功能的不二选择.

作为智慧建造中的基本力学构件, 功能梯度梁的动力学行为分析尤为重要. 特别是在装配式智慧建造过程中, 功能梯度梁运输及吊装过程的横向振动特性对运输和吊装过程的稳定性影响显著. Sankar^[5]基于 Euler-Bernoulli 梁理论, 得到了横向载荷作用下功能梯度梁弹性范围内的解. Reddy^[6]基于 von Karman 几何非线性理论, 建立了功能梯度梁的非线性 Euler-Bernoulli 梁模型和 Timoshenko 梁模型. 丁虎^[7]、王忠民等^[8]轴向运动功能梯度梁振动模型, 并分别采用伽辽金法和微分求积法分析其振动特性, 为本文分析功能梯度梁横向振动过程

奠定了基础. 刘金建等^[9]基于 Euler 梁理论研究了轴向运动功能梯度粘弹性梁横向振动的稳定性问题. Balireddy 和 Pitchaimani^[10]分析了时变轴向载荷作用下功能梯度梁振动特性及稳定性.

从本质上讲, 功能梯度梁的材料非均匀性和梁式结构的轴向运动均属于动力学对称破缺^[11]因素. 对于含有对称破缺因素的动力学系统, 本课题组基于多辛分析方法, 建立了广义多辛分析方法^[12]这一保结构理论框架, 并解决了一系列复杂动力学问题^[13-16]. 因此, 本文将基于保结构思想, 分析轴向运动功能梯度梁的横向振动频率特性, 为功能梯度梁的横向振动控制提供参考.

1 轴向运动功能梯度梁横向振动模型

本节参考文献[8, 9], 简要回顾轴向运动功能梯度梁横向振动动力学模型的建立过程. 考虑一轴向运动的简支功能梯度矩形截面梁(图1), 梁长度为 L , 横截面宽度为 b 、高为 h , 轴向运动速度为定常速度, 大小为 η . 为了刻画材料特性沿界面高度方向的梯度, 假定功能梯度材料有效杨氏模量和有效

2022-08-20 收到第1稿, 2022-09-28 收到修改稿.

* 国家自然科学基金资助项目(12172281, 11972284), 基础加强173计划基金项目(2021-JCJQ-JJ-0565), 陕西省科技创新团队资助(2022TD-61)和陕西高校青年教师创新团队资助

† 通信作者 E-mail: wphu@nwpu.edu.cn

密度均为 z 坐标的函数, 即 $E(z)$ 和 $\rho(z)$.

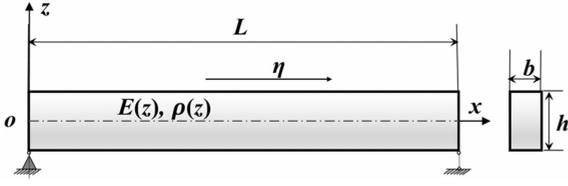


图1 轴向运动功能梯度梁的物理模型

Fig.1 Physical model of functionally graded beam with an axial velocity

以含两种组分(如金属材料 and 陶瓷材料)的功能梯度材料为例, 其有效材料参数可表述为:

$$\begin{aligned} E(z) &= (E_c - E_m)(z/h + 1/2)^k + E_m \\ &= E_m [(\beta_E - 1)(z/h + 1/2)^k + 1] \\ \rho(z) &= (\rho_c - \rho_m)(z/h + 1/2)^k + \rho_m \\ &= \rho_m [(\beta_\rho - 1)(z/h + 1/2)^k + 1] \end{aligned} \quad (1)$$

其中 E_c, E_m, ρ_c, ρ_m 分别为两种材料组分的物理参数, $\beta_E = E_c/E_m, \beta_\rho = \rho_c/\rho_m, k$ 为梯度指标. 需要说明的是, 从式(1)即可推导出功能梯度梁的中性层与几何对称中心重合.

基于 Euler-Bernoulli 梁基本假设, 依据文献[8], 功能梯度梁上任意点的位移可由梁轴线上任意点的轴向位移 $u(x, t)$ 和横向位移 $w(x, t)$ 表述:

$$\begin{aligned} u_x(x, z, t) &= u(x, t) - z\partial_x w(x, t) + \eta t \\ u_z(x, z, t) &= w(x, t) \end{aligned} \quad (2)$$

功能梯度梁上任意点的正应变分量和正应力分量分别为:

$$\begin{aligned} \varepsilon_x &= \partial_x u - z\partial_{xx} w \\ \sigma_x &= E(z)\varepsilon_x = E(z)(\partial_x u - z\partial_{xx} w) \end{aligned} \quad (3)$$

由其描述的梁的应变能可表述为:

$$\begin{aligned} U &= \frac{1}{2} \int_0^L \int_A \sigma_x \varepsilon_x dA dx \\ &= \frac{1}{2} \int_0^L [D_1 (\partial_x u)^2 - 2D_2 \partial_x u \partial_{xx} w + \\ &\quad D_3 (\partial_{xx} w)^2] dx \end{aligned} \quad (4)$$

其中, A 为梁的横截面面积, 并且:

$$(D_1, D_2, D_3) = \int_A E(z)(1, z, z^2) dA$$

功能梯度梁上任意点两个方向的速度分量分别为:

$$\begin{aligned} v_x &= \partial_t u_x(x, z, t) \\ &= \partial_t u(x, t) - z\partial_{tx} w(x, t) + \eta \\ v_z &= \partial_t w(x, t) + \eta \partial_x w(x, t) \end{aligned} \quad (5)$$

由此描述的梁的动能可表述为:

$$\begin{aligned} K &= \frac{1}{2} \int_0^L \int_A \rho(z) (v_x^2 + v_z^2) dA dx = \\ &= \frac{1}{2} \int_0^L \{ I_1 [(\partial_t u)^2 + \eta^2 + 2\eta \partial_t u + (\partial_t w)^2 + \\ &\quad \eta^2 (\partial_x w)^2 + 2\eta \partial_t w \partial_{tx} w] - 2I_2 \eta \partial_{tx} w - \\ &\quad 2I_2 \partial_t u \partial_{tx} w + I_3 (\partial_{tx} w)^2 \} dx \end{aligned} \quad (6)$$

其中

$$(I_1, I_2, I_3) = \int_A \rho(z) (1, z, z^2) dA$$

由哈密顿原理, 忽略梁的轴向惯性力及其由轴向惯性力诱导的横向分布载荷项, 并消去轴向位移项, 得到轴向运动功能梯度梁横向振动方程:

$$\begin{aligned} (D_3 - \frac{D_2^2}{D_1}) \partial_{xxxx} w - (I_3 - I_2 \frac{D_2}{D_1}) \partial_{xxx} w + \\ I_1 (\partial_{tt} w + \eta^2 \partial_{xx} w + 2\eta \partial_{tx} w) = 0 \\ \text{with } \begin{cases} w(0, t) = 0 & w(L, t) = 0 \\ \partial_{xx} w(0, t) = 0 & \partial_{xx} w(L, t) = 0 \end{cases} \end{aligned} \quad (7)$$

2 振动模型的近似对称形式及保结构离散

引入如下中间变量: $\partial_t w = \partial_x \psi = \frac{D_1 \varphi - D_1 I_2 \chi}{D_2 I_2 - D_1 I_3}, \partial_x w = \varphi, \partial_x \chi = \varphi$, 并定义状态向量: $\mathbf{z} = (w, \varphi, \chi, \psi, \varphi)^T$, 轴向运动功能梯度梁横向振动方程(不含边界条件)可以写成如下近似一阶对称形式:

$$\mathbf{M} \partial_t \mathbf{z} + \mathbf{K} \partial_x \mathbf{z} = \nabla_z S(\mathbf{z}) + \boldsymbol{\tau}(\mathbf{z}) \quad (8)$$

其中, $\mathbf{M}, \mathbf{K} \in \mathbf{R}^{5 \times 5}$ 为反对称矩阵:

$$\mathbf{M} = \begin{bmatrix} 0 & 0 & 0 & 0 & 1 \\ 0 & 0 & 0 & 0 & 0 \\ 0 & 0 & 0 & 0 & 0 \\ 0 & 0 & 0 & 0 & 0 \\ -1 & 0 & 0 & 0 & 0 \end{bmatrix},$$

$\mathbf{K} =$

$$\begin{bmatrix} 0 & D_3 - \frac{D_2^2}{D_1} & 0 & 0 & 1 \\ \frac{D_2^2}{D_1} - D_3 & 0 & 0 & 0 & 0 \\ 0 & 0 & 0 & I_2 \frac{D_2}{D_1} - I_3 & 0 \\ 0 & 0 & I_3 - I_2 \frac{D_2}{D_1} & 0 & 0 \\ 0 & 0 & 0 & 1 & 0 \end{bmatrix}$$

拟哈密顿函数为:

$$S(\mathbf{z}) = -\frac{1}{2} [I_1 \eta^2 w^2 + (D_3 - \frac{D_2^2}{D_1}) \varphi^2 -$$

$$I_1 \dot{\chi}^2 + (I_3 - I_2 \frac{D_2}{D_1}) \psi^2]$$

余项为: $\tau(z) = [-2I_1 \eta \psi, 0, \varphi, 0, 0]^T$.

与标准的多辛形式不同,近似对称形式含有如下对称破缺因素^[11]:

① 系数矩阵 M, K 及哈密顿函数 $S(z)$ 显含空

$$K = \underbrace{\begin{bmatrix} 0 & D_3 - \frac{D_2^2}{D_1} & 0 & 0 & 1/2 \\ \frac{D_2^2}{D_1} - D_3 & 0 & 0 & 0 & 0 \\ 0 & 0 & 0 & I_2 \frac{D_2}{D_1} - I_3 & 0 \\ 0 & 0 & I_3 - I_2 \frac{D_2}{D_1} & 0 & -1/2 \\ -1/2 & 0 & 0 & 1/2 & 0 \end{bmatrix}}_{\widehat{K}} + \underbrace{\begin{bmatrix} 0 & 0 & 0 & 0 & 1/2 \\ 0 & 0 & 0 & 0 & 0 \\ 0 & 0 & 0 & 0 & 0 \\ 0 & 0 & 0 & 0 & 1/2 \\ 1/2 & 0 & 0 & 1/2 & 0 \end{bmatrix}}_{\widetilde{K}}$$

①和③两个对称破缺因素引起的横向振动模型多辛结构残差和局部能量耗散均可以参照文献[11]显式给出,第②个对称破缺因素在模拟仿真中的处理方式可参照参考文献[17]进行.为避免与已有工作重复,在此不给出详细表达式和具体处理步骤,只在模拟结果中给出离散的多辛结构残差,以间接证明后续构造算法的有效性和保结构性能.

在梁长度方位内($0 \leq x \leq L$)采用空间步长进行均匀划分单元,并对系统采用时间步长进行 Preissmann 离散,得到保结构差格式:

$$M \delta_i^+ z_{i+1/2}^j + K \delta_x^+ z_i^{j+1/2} = \nabla_z S(z_{i+1/2}^{j+1/2}) + \tau(z_{i+1/2}^{j+1/2}) \quad (9)$$

其中: $z_{i+1/2}^{j+1/2} = \frac{1}{4}(z_i^j + z_{i+1}^j + z_i^{j+1} + z_{i+1}^{j+1})$, δ_x^+, δ_t^+ 均为一阶前向差分.

限于篇幅,格式的展开形式和消参后的形式不再给出,同时,离散的多辛结构残差和离散的局部能量耗散项也不再列出.需要强调的是,多辛结构残差是衡量格式保结构性能的重要依据,后续在数值结果中会详细讨论.

3 数值算例

为了将结果与文献[8, 9]的部分结果进行对比,材料参数取值如下: $E_c = 390\text{GPa}$, $E_m = 210\text{GPa}$, $\rho_c = 3960\text{kg/m}^3$, $\rho_m = 7800\text{kg/m}^3$.

为保证数值格式的保结构性能,依照广义多辛

间变量;

② 哈密顿函数梯度存在余项 $\tau(z)$;

③ 系数矩阵 M 非严格地反对称,因此将其分解

理论^[12],需要选取合适的时间步长使得在每一时间步内,离散的多辛结构绝对残差不超过差分格式的数值截断误差,即 $|\Delta_i| \leq o(\Delta t, \Delta x)$,其中 $o(\Delta t, \Delta x)$ 为格式的数值截断误差.为了计算方便,忽略高阶项并取 $\Delta t/\Delta x = 0.5$ 后,可以将数值截断误差上限估计值近似取为:

$$o(\Delta t, \Delta x) \leq [o] = 7\Delta t^2 \quad (10)$$

在考虑梯度指标取值较大的情形下,确定容许的最大时间步长.取 $k = 10^5$,将时间步长取值从 $\Delta t = 0.001\text{s}$ 逐渐增大,当式(10)刚好严格满足时,得到最大允许时间步长为 $\Delta t = 0.064\text{s}$,此时的多辛结构残差与数值截断误差上限估计值之间的关系如图2所示.因此,在后续模拟过程中,取时间步长为 $\Delta t = 0.05\text{s}$,空间步长为 $\Delta x = 0.1\text{m}$,就能保证所构造的格式具有良好的保结构性能.

分别取 $k = 0.001, 100$ 两种梯度指标,分别采用微分求积法(DQM)^[8]、复模态法(CMM)^[9]和保结构方法(SPM)模拟轴向运动功能梯度梁的横向振动过程,得到梁的前六阶频率值如表1所示.

从表1中不难发现,采用保结构分析方法得到的结果与复模态法得到的结果整体吻合较好.

随着频率阶次升高,复模态法和保结构方法得到的频率结果明显低于微分求积法得到的结果.考察微分求积法的求解过程,可知微分求积法得到的结果产生以上偏差的主要原因在于以下两个方面:① 在进行微分求积运算之前,将偏微分方程化为常微分方程过程中,只考虑了方程解的一阶频率分

量而忽略了高阶频率分量;②微分求积法采用非均匀网格离散,无法判断每一时间步内不等式($|\Delta_i| \leq o(\Delta t, \Delta x)$)的满足情况,不具有评价其保结构性能的条件.复模态法在一定程度上克服了上述两方面的问题,故得到的结果与本文保结构方法得到的结果吻合较好.上述结果表明,复模态法和保结构方法在分析轴向运动功能梯度梁横向振动问题中均具有较好的数值精度.

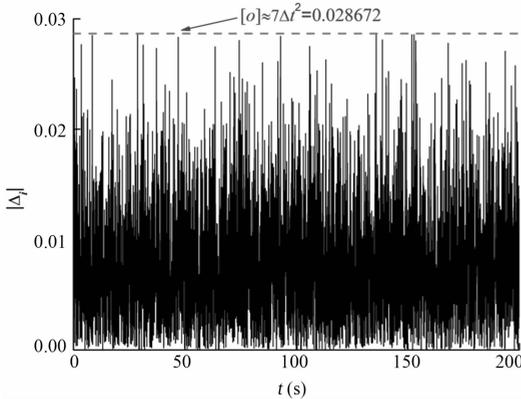


图2 轴向运动功能梯度梁的物理模型
Fig.2 Evolution of the absolute residual of the multi-symplectic structure

表1 前六阶频率结果对比 (Hz)

Table 1 Comparison of the first six frequencies (Hz)

k	Mode No.	DQM	CMM	SPM
0.001	1st	18.0385	18.0385	18.0385
	2nd	72.5801	72.5339	72.5339
	3rd	161.1975	160.0018	160.0018
	4th	289.8806	286.2147	286.2142
	5th	458.9380	452.7311	452.7096
	6th	666.2039	659.9018	659.3089
100	1st	9.7849	9.7849	9.7848
	2nd	32.9091	32.2286	32.2259
	3rd	80.3610	78.4392	78.4298
	4th	148.1315	144.3618	143.8100
	5th	237.2027	231.2156	230.9035
	6th	346.7738	338.8033	338.3271

4 结论

基于动力学系统的对称破缺理论和广义多辛分析方法,本文针对轴向运动功能梯度梁横向振动的动力学模型,发展了保结构分析方法,并用于分析轴向运动功能梯度梁横向振动的频率分布情况.研究表明:本文构造的数值求解算法在求解步长满足给定条件时具有良好的保结构性能,得到的

前六阶频率值与复模态法得到的结果吻合较好,同时分析了微分求积法得到的结果与保结构方法和复模态法得到的结果有明显差距的原因,为微分求积法的进一步改进指明了方向,也为轴向运动功能梯度梁横向振动这类复杂动力学问题的求解提供了新途径.

参 考 文 献

- Reddy J N, Chin C D. Thermomechanical analysis of functionally graded cylinders and plates. *Journal of Thermal Stresses*, 1998, 21(6):593 ~ 626
- Naebe M, Shirvanimoghaddam K. Functionally graded materials: a review of fabrication and properties. *Applied Materials Today*, 2016, 5:223 ~ 245
- Bartlett N W, Tolley M T, Overvelde J T B, et al. A 3D-printed, functionally graded soft robot powered by combustion. *Science*, 2015, 349(6244):161 ~ 165
- Tuan A N, Aiello M. Energy intelligent buildings based on user activity: a survey. *Energy and Buildings*, 2013, 56:244 ~ 257
- Sankar B V. An elasticity solution for functionally graded beams. *Composites Science and Technology*, 2001, 61(5):689 ~ 696
- Reddy J N. Microstructure-dependent couple stress theories of functionally graded beams. *Journal of the Mechanics and Physics of Solids*, 2011, 59(11):2382 ~ 2399
- Ding H, Chen L Q. Galerkin methods for natural frequencies of high-speed axially moving beams. *Journal of Sound and Vibration*, 2010, 329(17):3484 ~ 3494
- 姚晓莎, 王忠民, 赵凤群. 轴向运动功能梯度梁的横向振动. *机械工程学报*, 2013, 49(23):117 ~ 122 (Yao X S, Wang Z M, Zhao F Q. Transverse vibration of axially moving beam made of functionally graded materials. *Journal of Mechanical Engineering*, 2013, 49(23):117 ~ 122 (in Chinese))
- 刘金建, 蔡改改, 谢锋, 等. 轴向运动功能梯度粘弹性梁横向振动的稳定性分析. *动力学与控制学报*, 2016, 14(6):533 ~ 541 (Liu J J, Cai G G, Xie F, et al. Stability analysis on transverse vibration of axially moving functionally graded viscoelastic beams. *Journal of Dynamics and Control*, 2016, 14(6):533 ~ 541 (in Chinese))
- Balireddy S N, Pitchaimani J. Stability and dynamic behaviour of bi-directional functionally graded beam subjected to variable axial load. *Materials Today Communications*, 2022, 32: 104043
- Hu W, Wang Z, Zhao Y, et al. Symmetry breaking of infinite-dimensional dynamic system. *Applied Mathematics Letters*, 2020, 103:106207

- 12 Hu W P, Deng Z C, Han S M, et al. Generalized multi-symplectic integrators for a class of hamiltonian nonlinear wave PDEs. *Journal of Computational Physics*, 2013, 235:394 ~ 406
- 13 宋明哲, 邓子辰, 赵云平, 等. 含弱阻尼空间结构的耦合动力学保结构分析. *动力学与控制学报*, 2019, 17(5):419 ~ 424 (Song M Z, Deng Z C, Zhao Y P, et al. Coupling dynamic structure-persevering analysis of spatial structure with weak damping. *Journal of Dynamics and Control*, 2019, 17(5):419 ~ 424 (in Chinese))
- 14 Hu W, Huai Y, Xu M, et al. Mechano-electrical flexible hub-beam model of ionic-type solvent-free nanofluids. *Mechanical Systems and Signal Processing*, 2021, 159: 107833
- 15 Hu W, Xu M, Song J, et al. Coupling dynamic behaviors of flexible stretching hub-beam system. *Mechanical Systems and Signal Processing*, 2021, 151: 107389
- 16 Hu W, Xu M, Zhang F, et al. Dynamic analysis on flexible hub-beam with step-variable cross-section. *Mechanical Systems and Signal Processing*, 2022, 180:109423
- 17 Hu W P, Deng Z C, Wang B, et al. Chaos in an embedded single-walled carbon nanotube. *Nonlinear Dynamics*, 2013, 72(1-2):389 ~ 398

STRUCTURE-PRESERVING ANALYSIS ON TRANSVERSE VIBRATION OF FUNCTIONALLY GRADED BEAM WITH AN AXIAL VELOCITY *

Liu Tao¹ Zhou Yangxin² Hu Weipeng^{2†}

(1. Yulin City Investment Construction Development Co., Ltd., Yulin 719000, China)

(2. School of Civil Engineering and Architecture, Xi'an University of Technology, Xi'an 710048, China)

Abstract The axial velocity and the material's heterogeneity introduce the great challenge on the vibration analysis of the functionally graded beam with an axial velocity. In this work, the dynamic model of the transverse vibration of the functionally graded beam with an axial velocity is reviewed in brief firstly. Based on the dynamic symmetry breaking theory and the generalized multi-symplectic method for the infinite-dimensional system, a structure-preserving numerical scheme for the dynamic model is developed. In the numerical simulation, the critical step length satisfying the generalized multi-symplectic condition is obtained with the given material parameters. The first six frequencies of the transverse vibration model are presented employing the differential quadrature method, the complex modal method and the structure-preserving method respectively. From the numerical results, it can be found that the first six frequencies obtained by using the structure-preserving method are highly consistent with those obtained by using the complex modal method. To improve the precision of the differential quadrature method, the main factors resulting in the error are investigated. The main contribution of this work is proposing a new approach to analyze the complex dynamic problem like the transverse vibration of the functionally graded beam with an axial velocity considered in this paper.

Key words structure-preserving, functionally graded beam with an axial velocity, symmetry breaking, generalized multi-symplectic, transverse vibration

Received 20 August 2022, revised 28 September 2022.

* The project supported by the National Natural Science Foundation of China (12172281, 11972284), Foundation Strengthening Programme Technical Area Fund (2021-JCJQ-JJ-0565), the Fund of the Science and Technology Innovation Team of Shaanxi (2022TD-61) and Fund of the Youth Innovation Team of Shaanxi Universities

† Corresponding author E-mail: wphu@nwpu.edu.cn